Proceedings of the Institution of Mechanical Engineers, Part G: Journal of Aerospace Engineering
http://pig.sagepub.com/

A spline wavelet collocation method for the optimal control of flexible spacecraft

Qingbin Zhang, Zhiwei Feng, Qiangang Tang and Macdonald Malcolm

Proceedings of the Institution of Mechanical Engineers, Part G: Journal of Aerospace Engineering published online 31 March 2014
DOI: 10.1177/0954410014528885

Original Article

Institution of MECHANICAL ENGINEERS

Journal of AEROSPACE ENGINEERING

Proc IMechE Part G: J Aerospace Engineering
0(0) 1–9

DOI: 10.1177/0954410014528885
uk.sagepub.com/jaero
SAGE

A spline wavelet collocation method for the optimal control of flexible spacecraft

Qingbin Zhang[1], Zhiwei Feng[1], Qiangang Tang[1] and Macdonald Malcolm[2]

Abstract

A spline wavelet collocation method is presented to solve optimal control problem (OCP) of flexible spacecraft, which is often required to reorient and reposition with minimum manoeuvre time or fuel consumption. It is very difficult and computationally expensive to determine the open-loop optimal control inputs for flexible spacecraft, because the optimal control profile is often characterised by discontinuities or switching in the control variables. In our approach, the state and control variables are expanded via cubic spline wavelet decomposition, and then an OCP would be converted into a nonlinear programming problem where the wavelet coefficients are treated as the optimisation variables. As opposed to the usual pseudospectral method based on polynomial approximation, the wavelet advantageous properties of compact representation would inherently make it efficiently and accurately to solve nonlinear programming problem using standard solver. The novel approach is demonstrated by two typical optimal problems. The results show that our approach outperforms Gauss pseudospectral method for discontinuous OCPs arising from the flexible spacecraft.

Keywords

Wavelet collocation method, optimal control problem, spline wavelet, direct method, flexible spacecraft

Date received: 6 September 2013; accepted: 28 February 2014

Introduction

Flexible spacecrafts, including robotic manipulators, are often required to reorientate as quickly as possible with either minimum manoeuvre time or fuel consumption. Related control problems have attracted significant attention for more than three decades.[1,2] An elegant and useful input-shaping scheme was proposed by Smith and Singer.[3,4] A robust control approach for linear, time-invariant control systems was presented by Wie.[5] Nevertheless, for general rest-to-rest problems, with strong nonlinear dynamics and state/control constraints, the solution of realistic trajectory optimisation problems remains a highly complex problem. Moreover, the optimal control profile is often characterised by discontinuities or switching in the control variables, meaning that localised structures or sharp transitions can be lost in the control profile. As such, it remains difficult and computationally expensive to find the exact optimal solution for open loop control design.

For the flexible robot, the time optimal point-to-point trajectory planning of a flexible link robot is conducted with an exact feedforward linearisation in combination with a feedback part by Springer et al.[6] An indirect method is employed to solve the problem of time-optimal trajectory planning of robot manipulators in point-to-point motion.[7] As far as the authors know, the open loop optimal control method used in the above literature is rarely used for the flexible spacecraft especially with low first mode frequency.

The derivation of analytical solutions to the optimal control problem (OCP) is unattainable for all but a limited number of highly constrained scenarios. As a result, numerical techniques are typically adopted, which are generally computationally extensive. Betts and Rao had provided an excellent survey of the numerical methods for OCP.[8,9] Numerical methods for solving the OCP can be largely divided into two major categories: indirect methods and direct methods.[8] In the indirect method, calculus of variation is used to determine the first order optimality conditions of the OCP, resulting in a multiple-point boundary-value problem. In the direct method, the state and/or control of OCP is discretised in some special manner,

[1]College of Aerospace Science and Engineering, National University of Defense Technology, Changsha, Hunan, P.R. China
[2]Advanced Space Concepts Laboratory, University of Strathclyde, Glasgow, Scotland, UK

Corresponding author:
Qingbin Zhang, College of Aerospace Science and Engineering, National University of Defense Technology, Changsha, Hunan, P.R. China.
Email: qingbinzhang@sina.com

then the original OCP is transcribed to a nonlinear programming problem (NLP) that can be solved via the well-known optimisation techniques, such as SQP and SNOPT.[10] The popular direct methods to solve OCP are pseudospectral (PS) methods. Since PS methods use global orthogonal polynomials to parameterise the state and control, it would be very computationally expensive to cope with the non-smooth OCP arising from practical flexible spacecraft manoeuvres.

Wavelet multi-resolution approximation should be a desirable way to solve OCP with discontinuities or switching in the control variables. As a novel attractive numerical technique, wavelet multi-resolution approximation seems to combine the advantages of both spectral and finite element methods, and has attracted much attention as a potential efficient numerical technique for approximating function with singularities.[11–13] In fact, wavelet approximation has been widely used in numerous areas of applied mathematics as diverse as signal analysis, image processing and solving partial differential equation (PDE), and has significantly impacted many areas of science and engineering. More recently, Dai used the Haar wavelet technique as a method for discretising the nonlinear system equations for OCPs.[14] In this paper, a direct method for solving OCP is presented based on spline wavelet collocation method (SWCM). In our approach, unlike the pseudospectral method based on polynomial approximation, the basic idea is to expand the state and control variables via cubic spline wavelet decomposition. Therefore, the advantageous properties of compact representation of the wavelet could make it efficient and accurate to solve the OCP. The novel approach is demonstrated by two typical optimal control problems.

The remainder of the paper is organised as follows. The next section gives a brief introduction to the cubic spline wavelet, including wavelet approximation and derivative matrixes. In the Discretization of OCP section, the approach to convert continuous OCP of flexible spacecraft to NLP is presented. In the Simulation section, the features and benefits of the approach are demonstrated by two examples of flexible spacecraft. Finally, the conclusion of the paper is provided.

Interval spline wavelet and function approximation

Cubic spline wavelets are employed in our approach, as they are capable of dealing with boundary conditions and analytically expressed. For completeness, the definition of interval spline wavelet is briefly reviewed. A comprehensive survey about spline wavelet can be found in the literatures.[15–17]

Let $I=[0,L]$ denote a finite interval (for the sake of simplicity, it is assumed that the integer $L>4$). $H_0^2(I)$ and $H^2(I)$ denote the following two

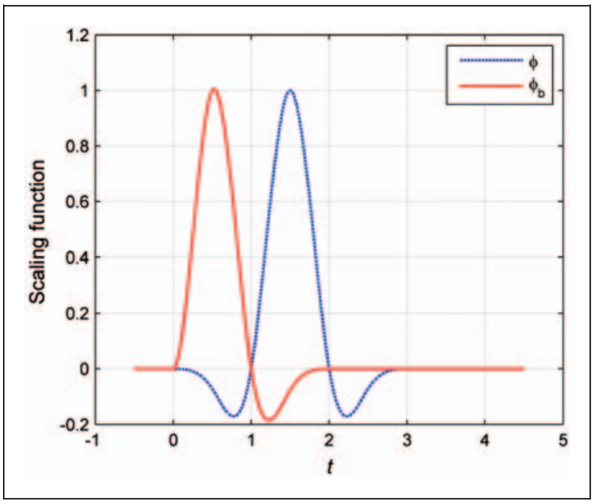

Figure 1. Scaling functions.

Sobolev spaces with finite L^2 up to the second order derivative, i.e

$$H^2(I)=\left\{f(t),t\in I\middle|\left\|f^{(i)}\right\|_2<\infty, i=0,1,2\right\} \tag{1}$$

$$H_0^2(I)=\left\{\begin{matrix} f(t), f\in H^2(I)| \\ f(0)=f'(0)=f(L)=f'(L)=0\end{matrix}\right\} \tag{2}$$

The interior scaling function $\phi(t)$ and boundary scaling function $\phi_b(t)$, illustrated in Figure 1, are specially designed as follows

$$\phi(t)=\frac{1}{6}\sum_{j=0}^{4}\binom{4}{j}(-1)^j(t-j)_+^3 \tag{3}$$

$$\phi_b(x)=\frac{3}{2}t_+^2-\frac{11}{12}t_+^3+\frac{3}{2}(t-1)_+^3-\frac{3}{4}(t-2)_+^3 \tag{4}$$

where

$$t_+^n=\begin{cases}0 & t<0\\ t^n & t\geqslant 0\end{cases}$$

In order to construct a wavelet decomposition of Sobolev space $H_0^2(I)$, the interior wavelet function and boundary wavelet are designed as follows

$$\psi(t)=-\frac{3}{7}\phi(2t)+\frac{12}{7}\phi(2t-1)-\frac{3}{7}\phi(2t-2) \tag{5}$$

$$\psi_b(t)=\frac{24}{13}\phi_b(2t)-\frac{6}{13}\phi(2t) \tag{6}$$

Similar to the usual wavelet construction, the scaling and wavelet function can be dilated and translated as

$$\phi_{j,k}(t)=\phi\left(2^jt-k\right),\phi_{b,j}(t)=\phi_b\left(2^jt\right) \tag{7}$$

$$\psi_{j,k}(t)=\psi\left(2^jt-k\right),j\geqslant 0,k=0,\ \ldots,n_j-3 \tag{8}$$

$$\psi_{j,-1}(t)=\psi_b\left(2^jt\right),\psi_{j,n_j-2}(t)=\psi_b\left(2^j(L-t)\right) \tag{9}$$

where $n_j=2^jL$.

For any $j,k\in \boldsymbol{Z}$, the scale and wavelet spaces are defined as

$$V_j=span\left\{\phi_{j,k}(t)|0\leqslant k\leqslant\left(2^JL-4\right),\phi_{b,j}(t),\phi_{b,j}(L-t)\right\} \tag{10}$$

$$W_j=span\left\{\psi_{j,k}(t)|k=-1,\ \ldots,n_j-2\right\} \tag{11}$$

Thereafter, any function $f(t)\in H_0^2(I)$ can be approximated as close as possible by a function $P_Jf(t)\in V_J$ for a sufficiently large J, and $P_Jf(t)$ has a unique orthogonal decomposition as follows

$$\begin{aligned}&P_Jf(t)=I_{b,J}f+f_0+g_0+g_1+\cdots+g_{J-1}\\&\quad f_0\in V_0,g_i\in W_i,0\leqslant i\leqslant J\end{aligned} \tag{12}$$

In general, f_0 is the coarsest approximation, each g_j represents the fluctuation of $f(t)$ between the two successive levels of resolution j and $j+1$, and the magnitude of wavelet coefficients would also reflect the local scale and changes of the function to be approximated.

In practice, two splines η_1 and η_2 are used to handle non-homogeneity of the boundary conditions

$$\eta_1(t)=(1-t)_+^3 \tag{13}$$

$$\eta_2(t)=2t_+-3t_+^2+\frac{7}{6}t_+^3-\frac{4}{3}(t-1)_+^3+\frac{1}{6}(t-2)_+^3 \tag{14}$$

Furthermore, an interpolating spline $I_{b,j}f(t)$, $j\geqslant 0$ can be designed as follows

$$\begin{aligned}I_{b,j}f(t)=&f(0)\eta_1\left(2^jt\right)+\left[\frac{x'(0)}{2^{j+1}}+\frac{3x(0)}{2}\right]\eta_2\left(2^jt\right)\\&+\left[\frac{x'(L)}{2^{j+1}}+\frac{3x(L)}{2}\right]\eta_2\left[2^j(L-t)\right]\\&+f[L]\eta_1\left[2^j(L-t)\right]\end{aligned} \tag{15}$$

It can be easily verified that $f(t)-I_{b,j}f(t)$ belongs to $H_0^2(I)$. In order to approximate $f(t)\in H^2(I)$ in the same form of equation (6), the scaling space V_0 and the wavelet space W_j are refined by employing the following basis functions[16]

$$\phi_{0,k}(t)=\phi(t-k),0\leqslant k\leqslant L-4 \tag{16}$$

$$\phi_{0,-3}(t)=\eta_1(t-k),\phi_{0,-2}(t)=\eta_2(t-k) \tag{17}$$

$$\phi_{0,-1}(t)=\phi_b(t-k),\phi_{0,L-3}(t)=\phi_b(L-t) \tag{18}$$

$$\phi_{0,L-2}(t)=\eta_2(L-t),\phi_{0,L-1}(t)=\eta_1(L-t) \tag{19}$$

$$\psi_{j,-1}(t)=\psi_{b0}\left(2^jt\right),\psi_{j,0}(t)=\psi_{b1}\left(2^jt\right) \tag{20}$$

$$\psi_{j,n_j-2}(t)=\psi_{b0}\left[2^j(L-t)\right],\psi_{j,n_j-1}(t)=\psi_{b0}\left[2^j(L-t)\right] \tag{21}$$

where

$$\begin{aligned}&\psi_{b0}(t)=-\frac{56}{99}\left[\psi_{0,-1}(t)+14\psi_{0,-2}(t)\right]\\&\psi_{b1}(t)=\frac{182}{181}\left[\psi(t)+\frac{1}{13}\psi_{0,-1}(t)+\frac{14}{13}\psi_{0,-2}(t)\right]\end{aligned} \tag{22}$$

The new spaces V_0 and W_j are defined as

$$V_0=span\left\{\phi_{j,k}(t)|-3\leqslant k\leqslant L-1\right\} \tag{23}$$

$$W_j=span\left\{\psi_{j,k}(t)|k=-1,\ \ldots,n_j-2\right\},0\leqslant j\leqslant J-1 \tag{24}$$

Using the refined spaces V_0 and W_j, any function $f(t)\in H^2(I)$ can be also decomposed in the form of

$$\begin{aligned}&P_Jf(t)=f_0+g_0+g_1+\cdots+g_J\\&\quad f_0\in V_0,g_i\in W_i,0\leqslant i\leqslant J\end{aligned} \tag{25}$$

which can approximate $f(t)$ as closely as required if J is large enough. For the sake of notation, $P_Jf(t)$ can be expanded in the form of

$$P_Jf(t)=I_{V_{b0}}f(t)+\sum_{j=0}^{J-1}I_{W_j}f(t) \tag{26}$$

where

$$I_{W_j}f(t)=\sum_{k=-1}^{n_j-2}\hat{f}_{j,k}\psi_{j,k}(t) \tag{27}$$

$$\begin{aligned}I_{V_{b0}}f(t)=&\hat{f}_{-1,-3}\eta_1(t)+\hat{f}_{-1,-2}\eta_2(t)+\hat{f}_{-1,-1}\phi_b(t)\\&+\sum_{k=0}^{L-4}\hat{f}_{-1,k}\phi_k(t)\hat{f}_{-1,L-3}\phi_b(L-t)\\&+\hat{f}_{-1,L-2}\eta_2(L-t)+\hat{f}_{-1,L-1}\eta_1(L-t)\end{aligned} \tag{28}$$

It is essential to choose a special series of collocations for V_0 and W_j, as this is crucial for the fast Discrete Wavelet Transform and to map the discrete sample values of a function to its wavelet expansions. The following wavelet collocation points are chosen for V_0

$$T^{(0)}=\left\{0,\frac{1}{2},1,2,\ \ldots,L-1,L-\frac{1}{2},L\right\}=\left\{t_k^{(0)}\right\} \tag{29}$$

along with the following ones for W_j

$$T^{(j)} = \left\{\frac{1}{2^{j+1}}, \frac{1}{2^j}, \ldots, L - \frac{1}{2^{j+1}}\right\} = \left\{t_k^{(j)}\right\}_{k=1}^{n_j-2} \tag{30}$$

The number of collocation points in V_0 and W_j are exactly $L+3$ and n_j, both matching the dimensions of space V_0 and W_j.

Discretization of OCP

In general, the equation of motion of flexible space structure system can be described by

$$\mathbf{M}(\boldsymbol{x})\ddot{\boldsymbol{x}} + \mathbf{C}(\boldsymbol{x}, \ddot{\boldsymbol{x}}) + \mathbf{K}\boldsymbol{x} = \mathbf{G}\boldsymbol{u}, \boldsymbol{t} \in \left[\boldsymbol{t}_0, \boldsymbol{t}_f\right] \tag{31}$$

where $\boldsymbol{x} \in R^{n_x}$ is a generalised displacement vector, $\mathbf{M}$ is the mass matrix, $\mathbf{K}$ is the stiffness matrix, $\mathbf{C}$ is the damping matrix, $\mathbf{G}$ is the control input distribution matrix, $\boldsymbol{u}$ is the control input vector, $\boldsymbol{t}_0$ is a fixed initial time and $\boldsymbol{t}_f$ is a free terminal time. In practical applications, some path constraints are often required and can be described as

$$\boldsymbol{H}_{\min} \leqslant \boldsymbol{H}[\boldsymbol{x}(t), \boldsymbol{u}(t)] \leqslant \boldsymbol{H}_{\max} \tag{32}$$

along with the boundary conditions

$$\boldsymbol{B}_{\min} \leqslant \boldsymbol{B}\left[\boldsymbol{x}(t_0), \boldsymbol{x}\left(t_f\right), t_f\right] \leqslant \boldsymbol{B}_{\min} \tag{33}$$

The objective of trajectory optimisation is to find a control input that minimises the performance index, described as

$$J = \phi\left[\boldsymbol{x}(t_0), \boldsymbol{x}(t_f), t_f\right] \tag{34}$$

The aforementioned OCP is often called Mayer problem, where the cost function has no integral term. In most cases, the cost function can be described as follows

$$J = \varphi\left[\boldsymbol{x}(t_0), \boldsymbol{x}(t_f), t_f\right] + \int_{t_0}^{t_f} f[\boldsymbol{x}(t), \boldsymbol{u}(t), t]dt \tag{35}$$

which is called Bolza problem. As a matter of fact, any Bolza problem can be converted into a Mayer problem by adding a new state.[18]

The direct approach for the continuous OCP is to discrete and transcribe equations (15)–(18) into a nonlinear programming (NLP) problem. The scheme presented herein is based on approximating the state and control trajectories using cubic spine wavelets, making it different from Gauss pseudospectral methods (GPM) which are based on interpolating polynomials.

For notational convenience, the projection of $f(t) \in H^2$ can be simply rewritten as follows

$$P_J f(t) = \sum_{k=1}^{N_J} \hat{f}_k \tilde{\phi}_k(t), \quad k = 1, \ldots, N_J \tag{36}$$

where $\hat{\boldsymbol{f}} = \{\hat{f}_k\}$ denotes all wavelet coefficients, $\tilde{\phi}_k(t)$ basis functions, $\{\tau_k\}$ the collocation points.

First, the time interval $t \in [t_0, t_f]$ is converted into $\tau \in [0, L]$ via transformation

$$\tau = L\frac{t - t_f}{t_0 - t_f} \tag{37}$$

Next, $\boldsymbol{X}$ and $\boldsymbol{U}$ are denoted as the values of state and control at all collocation points. The objective function can be rewritten as

$$J = \phi\left[\boldsymbol{X}_0, \boldsymbol{X}_{N_J}, t_f\right] \tag{38}$$

Next, the state can be approximated in the form of

$$\boldsymbol{x}(\tau) \approx \sum_{i=0}^{N_J} \hat{\boldsymbol{X}}_i \tilde{\phi}_i(\tau) \tag{39}$$

Additionally, the control can also be approximated as

$$\boldsymbol{u}(\tau) \approx \sum_{i=0}^{N_J} \hat{\boldsymbol{U}}_i \tilde{\phi}_i(\tau) \tag{40}$$

Since $\tilde{\phi}_i(\tau)$ is in the form of cubic spline function, of which the derivations can be easily obtained. The derivative of each basis function at the collocation points can be represented in the following matrix

$$D_{ki}^0 = \tilde{\phi}_i(\tau_k), \quad D_{ki}^1 = \frac{\mathrm{d}\tilde{\phi}_i(\tau_k)}{dt}, \quad D_{ki}^2 = \frac{d^2\tilde{\phi}_i(\tau_k)}{dt^2}$$
$$k, i = 1, \ldots, N_J \tag{41}$$

If $\boldsymbol{X}$ and $\boldsymbol{U}$ are denoted as the values of state and control at all collocation points, it is easy to obtain the following matrices

$$\begin{aligned} \boldsymbol{X} &= \sum_{i=1}^{N_J} D_{ki}^0 \hat{\boldsymbol{X}}_i, \quad \dot{\boldsymbol{X}} = \sum_{i=1}^{N_J} D_{ki}^1 \hat{\boldsymbol{X}}_i \\ \boldsymbol{X} &= \sum_{i=1}^{N_J} D_{ki}^2 \hat{\boldsymbol{X}}_i, \quad \boldsymbol{U} = \sum_{i=1}^{N_J} D_{ki}^0 \hat{\boldsymbol{U}}_i \end{aligned} \tag{42}$$

Consequently, the dynamics constraint can be transcribed into algebraic constraints via the differential approximation matrix as follows

$$\begin{aligned} \zeta_k = &\left[M\left(\sum_{i=1}^{N_J} D_{ki}^0 \hat{\boldsymbol{X}}_i, \sum_{i=1}^{N_J} D_{ki}^1 \hat{\boldsymbol{X}}_i\right)\right] \sum_{i=1}^{N_J} D_{ki}^2 \hat{\boldsymbol{X}}_i \\ &+ C\left(\sum_{i=1}^{N_J} D_{ki}^0 \hat{\boldsymbol{X}}_i, \sum_{i=1}^{N_J} D_{ki}^1 \hat{\boldsymbol{X}}_i\right) \\ &+ K\left(\sum_{i=1}^{N_J} D_{ki}^1 \hat{\boldsymbol{X}}_i\right) \hat{\boldsymbol{X}}_i - G \sum_{i=1}^{N_J} D_{ki}^0 \hat{\boldsymbol{U}}_i = 0, \quad k = 1, \ldots, N_J \end{aligned} \tag{43}$$

The path constraints can also be discretised as

$$\boldsymbol{H}_{\min} \leqslant h_k = \boldsymbol{H}\left[\sum_{i=1}^{N_J} D_{ki}^0 \hat{\boldsymbol{X}}_i, D_{ki}^0 \hat{\boldsymbol{U}}_i, t\right] \leqslant \boldsymbol{H}_{\max} \qquad (44)$$

$$k = 1, \ldots, N_J$$

Similarly, the boundary constraints can be rewritten as follows

$$\boldsymbol{B}_{\min} \leqslant b_k = \boldsymbol{B}\left(\sum_{i=1}^{N_J} D_{ki}\hat{\boldsymbol{X}}_i, \sum_{i=1}^{N_J} D_{ki}\hat{\boldsymbol{U}}_i; t_0, t_f, \right) \leqslant \boldsymbol{B}_{\max}$$

$$k = 1, \ldots, N_J \qquad (45)$$

For notational simplicity, $\{b_k\}$ is rewritten as vector B^{N_J}, $\{h_k\}$ as matrix H^{N_J} and $\{\zeta_k\}$ as $\{\Upsilon^{N_J}\}$. Finally, the continuous OCP of flexible spacecraft system can be converted into NLP as follows

$$\min\ F = \varphi[\boldsymbol{y}] \qquad (46)$$

subject to

$$\boldsymbol{G}_l \leqslant \boldsymbol{G}(\boldsymbol{y}) \leqslant \boldsymbol{G}_u, \quad \boldsymbol{y}_l \leqslant \boldsymbol{y} \leqslant \boldsymbol{y}_u \qquad (47)$$

where the decision vector $\boldsymbol{y}$ is constructed from wavelet coefficient as follows

$$\boldsymbol{y} = \begin{bmatrix} vec(\hat{\boldsymbol{X}}) \\ vec(\hat{\boldsymbol{U}}) \\ t_f \end{bmatrix}_{(n_x+n_u)N_J+1} \qquad (48)$$

The objective function is given by

$$F = \varphi[\boldsymbol{y}] = \varphi\left[\hat{\boldsymbol{X}}D_{k0}, \hat{\boldsymbol{X}}D_{kN_J}, t_f\right] \qquad (49)$$

while the constraint $G(\boldsymbol{y})$ is rewritten as

$$\boldsymbol{G}(\boldsymbol{y}) = \begin{bmatrix} vec(\Upsilon^{N_J}) \\ vec(H^{N_J}) \\ vec(B^{N_J}) \end{bmatrix}_{(n_x+n_u)N_J+1} \qquad (50)$$

The boundary condition can be rewritten as

$$\boldsymbol{G}_l = \begin{bmatrix} 0_{n_x N_J} \\ stack(H_{\min}, N_J) \\ stack(B_{\min}, N_J) \end{bmatrix}, \quad \boldsymbol{G}_r = \begin{bmatrix} 0_{n_x N_J} \\ stack(H_{\max}, N_J) \\ stack(B_{\max}, N_J) \end{bmatrix} \qquad (51)$$

and the bounds on decision are given by

$$\boldsymbol{y}_l = \begin{bmatrix} stack(-\infty, N_J) \\ stack(-\infty, N_J) \\ 0 \end{bmatrix}, \quad \boldsymbol{y}_r = \begin{bmatrix} stack(+\infty, N_J) \\ stack(+\infty, N_J) \\ +\infty \end{bmatrix} \qquad (52)$$

where, vec(A) forms a nm-column vector by vertically stacking the columns of the $n \times m$ matrix A, and $stack(x, n)$ creates a nm-column vector by stacking n copies of column m-vector x.

Simulation

In this section, the validity of the presented method is verified by a typical linear OCP with an analytical solution, and the efficiency is demonstrated by a nonlinear flexible spacecraft system.

Linear system

A simple rigid-body system is shown in Figure 2, which can represent a linear, time-invariant controllable system with bounded control input.[19]

The equation of motion of such a system is simply given by

$$m\ddot{x} = u \qquad (53)$$

where x is the position of the body, and the control force u is bounded as $|u| \leqslant u_a$. The rest-to-rest, time optimal solution control for $x(t_0) = \dot{x}(t_0) = \dot{x}(t_f) = 0$, $x(t_f) = x_f$ can be found in an analytical form of

$$u^*(t) = u_s(t) - 2u_s(t - 0.5t_f) + 2u_s(t - t_f) \qquad (54)$$

where

$$u_s(t) = \begin{cases} u_a & t \geqslant 0 \\ 0 & t < 0 \end{cases}, \quad t_f = \sqrt{2m/x_f} \qquad (55)$$

It is obvious that the time optimal control solution is of bang–bang function with one switch.

The system parameters are selected as $x_f = 1$, $m = 1$ with appropriate units. The numerical results compared to the true solution are shown in Figures 3 and 4 for two different resolution levels. It can be seen

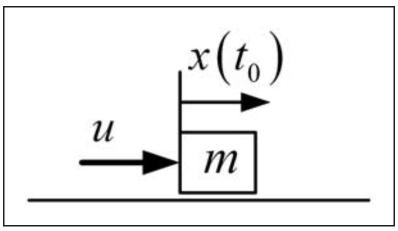

Figure 2. A simple rigid body system.

that in the domain with a singularity, the results from spline wavelet-collocation method (SWCM) can make little better approximation than GPM. In addition, the numerical results would be more and more accurate as the resolution level increases, which is in accordance with the feature of the multi-scale approximation. The overall computation time as well as the optimal result is given in Table 1. Clearly, the computation time of SWCM is less than GPM, while the optimal results are competitive with that obtained from GPM.

Nonlinear system

Consider a typical flexible spacecraft example, shown in Figure 5, which is a generic representation of spacecraft with flexible appendage.[20] J_b is the inertia of main body, m is the lumped mass, L is length of the massless rods, R is the distance from the mass center to the attachment point of the rods, θ is the main body angle relative to the inertial frame, θ_a is the appendage angle related to the main body, k is the torsional spring constant and T is the control torque bounded as $|T| \leqslant T_a$.

The goal is to minimise the manoeuvre time

$$J = t_f \tag{56}$$

The equation of motion of such a flexible-rigid system can be written as follows

$$\mathbf{M}\ddot{\boldsymbol{x}} + \mathbf{C}(\boldsymbol{x}, \dot{\boldsymbol{x}}) + \mathbf{K}\boldsymbol{x} = \mathbf{G}\boldsymbol{u} \tag{57}$$

Table 1. Optimal results from different approaches.

	Optimal results		Computation time	
Number of collocations	GPM	SWCM	GPM	SWCM
19	2.0043	2.0068	1.880650	0.07695
35	2.0013	2.0032	3.342077	0.192254
67	2.0004	2.0023	6.496522	0.413161

GPM: Gauss pseudospectral methods; SWCM: spline wavelet collocation method.

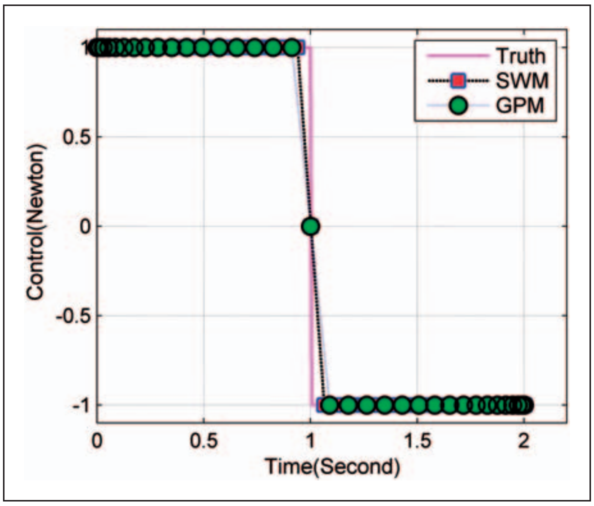

Figure 3. Time-optimal control input (using 35 collocations).

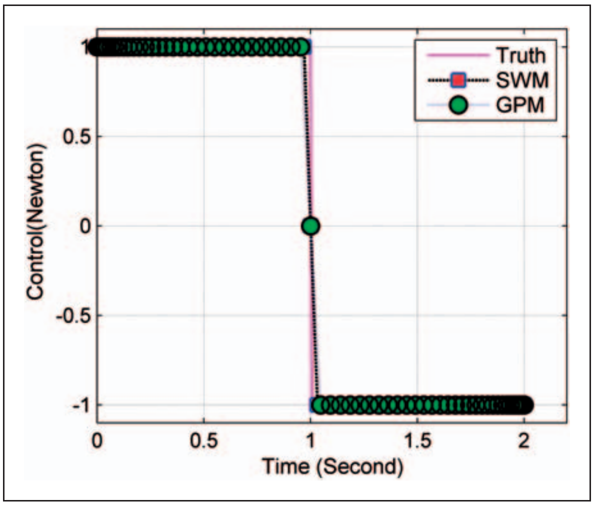

Figure 4. Time-optimal control input (using 67 collocations).

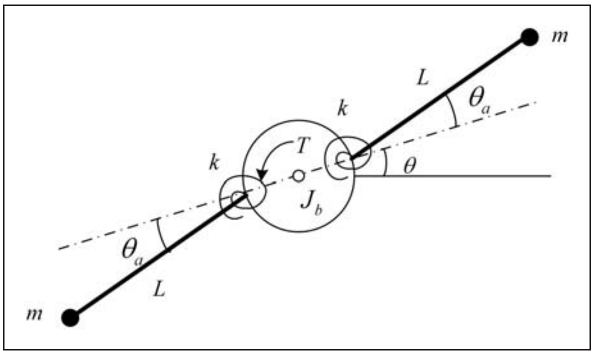

Figure 5. Flexible spacecraft system.

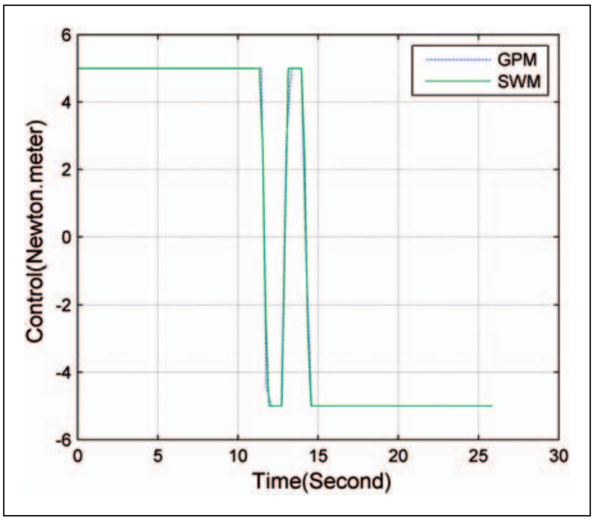

Figure 6. Time-optimal control torque input (131 points).

where

$$\boldsymbol{x} = [\theta, \theta_a]^T \tag{58}$$

$$\mathrm{M} = \begin{bmatrix} J_b + 2m(R^2 + L^2 + 2RL\cos\theta_a) & 2m(L^2 + RL\cos\theta_a) \\ 2m(L^2 + RL\cos\theta_a) & 2mL^2 \end{bmatrix} \tag{59}$$

$$\mathrm{C} = -2mRL\sin\theta_a \begin{bmatrix} \dot{\theta}_a - \dot{\theta} & \dot{\theta}_a \\ \dot{\theta}_a & 0 \end{bmatrix}, \quad \mathrm{K} = \begin{bmatrix} 0 & 0 \\ 0 & 2k \end{bmatrix} \tag{60}$$

$$\mathrm{G} = \begin{bmatrix} 1 & 0 \\ 0 & 0 \end{bmatrix}, \quad \boldsymbol{u} = \begin{bmatrix} T \\ 0 \end{bmatrix} \tag{61}$$

The boundary conditions are given as

$$\boldsymbol{x}(0) = [0, 0]^T, \quad \boldsymbol{x}(t_f) = \left[30^0, 0\right]^T \tag{62}$$

It is assumed that the nominal parameters are selected as $J_b = 440$, $R = 2.5$, $m = 10$, $L = 5$, $k = 100$ and $T_a = 5$ with appropriate units. It should be emphasised that such an OCP has no analytical solution, and the solution is very computationally expensive to obtain. A numerical solution with 131 and 259 collocation points is selected for this

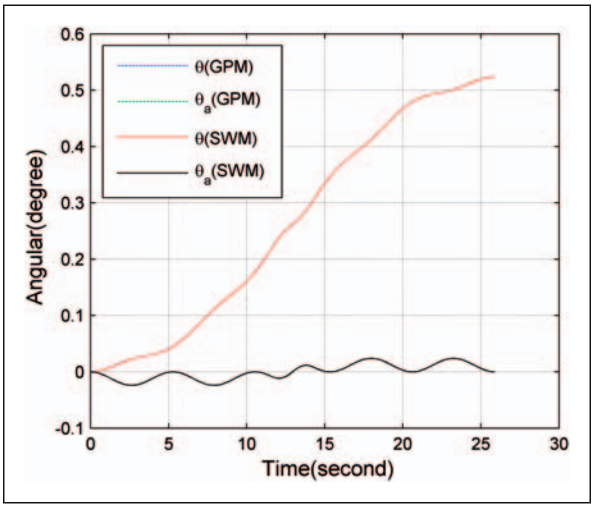

Figure 7. Angle responses to optimal control.

Table 2. Optimal results from different approaches.

	Optimal result		Computation time	
Number	GPM	SWCM	GPM	SWCM
131	25.86	25.97	16.74	15.85
259	25.86	25.92	38.54	35.21

GPM: Gauss pseudospectral methods; SWCM: spline wavelet collocation method.

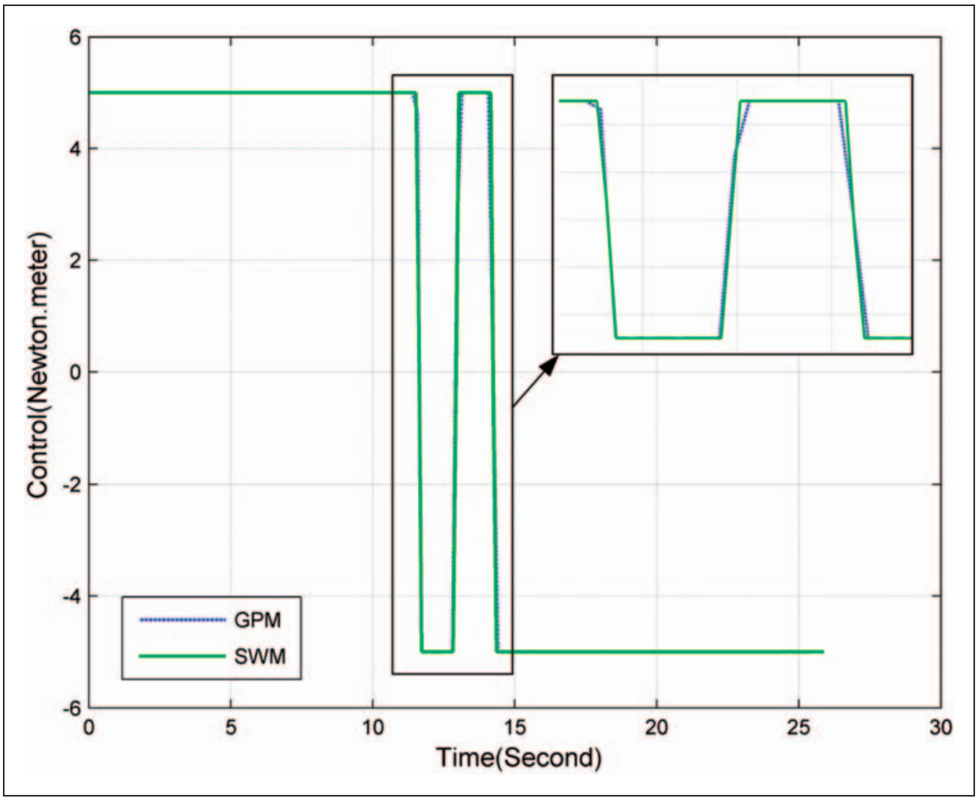

Figure 8. Time-optimal control torque input (259 points).

example. The time optimal control input is shown in Figure 6 and the time response of θ and θ_a to the optimal control (131 points) is shown in Figure 7. The optimal results along with computation time are given in Table 2. The simulations indicate that SWCM can accurately capture the switching times with little computational resource while optimal result from SWCM is almost the same as that from GPM. As can be seen in Figure 8, the result shows that the optimal control for the 259 points from SWCM is a little better than that for the GPM. As can be seen from the Table 2, for more points, the efficient of the SWCM is more obvious.

It is noted that in the nonlinear example of attitude manoeuvre of flexible spacecraft, only slight improvement in the calculation efficiency has been demonstrated, and the optimal result seems to be a little worse for 131 points. However, it is efficient and accurate in the linear example for the SWCM. The wavelet is suitable to approximate the functions with local sharp or singularity with higher accuracy. In the linear example, since there is only one switch, it is efficient with fewer points. In the nonlinear example, there are multiple local switches. Therefore, more points are required to get an efficient and accurate result. In the 259 points run illustrated in Figure 8, it can be observed that the accuracy is slightly improved than that of GPM, and the efficiency is more obvious.

Conclusion

The main objective of the paper was to present a new numerical direct method for solving the OCP of flexible spacecraft. The state and the control of original OCP are both expressed via cubic spline wavelets, and then the original OCP can be transcribed and converted into NLP in which the wavelet coefficients are treated as optimisation variables. Compared to other direct method for optimal control problem, the major advantage of this approach is that the switching time of control profile can be accurately captured with little computational resource. The proposed method is verified by a typical problem with analytical solution, and applied to the nonlinear flexible spacecraft system. The results illustrate that our approach outperforms general GPM for OCPs with discontinuities or switching in the control variables.

Funding

This work was supported by the National Natural Science Foundation of China (No. 11272345) and the Science Project of the National University of Defense Technology (No. GJ07-01-01 and No. JC13-01-04).

Conflict of interest

None declared.

Acknowledgements

The authors thank the anonymous reviewers for their invaluable comments on the draft of this paper. Their suggestions considerably improved the final version of the manuscript.

References

1. Hecht N and Junkins J. Near-minimum-time control of a flexible manipulator. *J Guidance Control Dynamics* 1992; 15: 477–481.
2. Singh T. Fuel/time optimal control of the benchmark problem. *J Guidance Control Dynamics* 1995; 18: 1225–1231.
3. Singhose W, Derezinski S and Singer N. Extra-insensitive input shapers for controlling flexible spacecraft. *J Guidance Control Dynamics* 1996; 19: 385–391.
4. Singhose W, Bohlke K and Seering W. Fuel-efficient pulse command profiles for flexible spacecraft. *J Guidance Control Dynamics* 1996; 19: 954–960.
5. Bong W, Sinha R and Liu Q. Robust time-optimal control of uncertain structural dynamic systems. *J Guidance Control Dynamics* 1993; 16: 980–983.
6. Springer K, Gattringer H and Staufer P. On time-optimal trajectory planning for a flexible link robot. *Proc IMechE, Part I: J Systems and Control Engineering* 2013; 227: 752–763.
7. Ghasemi MH, Kashiri N and Dardel M. Time-optimal trajectory planning of robot manipulators in point-to-point motion using an indirect method. *Proc IMechE, Part C: J Mechanical Engineering Science* 2011; 226: 473–484.
8. Rao A. A survey of numerical methods for optimal control. *Adv Astronaut Sci* 2009; 135: 497–528.
9. Betts J. Survey of numerical methods for trajectory optimization. *J Guidance Control Dynamics* 1998; 21: 193–207.
10. Gill P, Murray W and Saunders M. SNOPT: An SQP algorithm for large–scale constrained optimization. *SIAM Rev* 2005; 47: 99–131.
11. Schneide K and Vasilyev O. Wavelet methods in computational fluid dynamics. *Ann Rev Fluid Mech* 2010; 42: 473–483.
12. Vasilyev OV, Yuen D and Paolucci S. Solving PDEs using wavelets. *Comput Phys* 1997; 11: 429–435.
13. Vasilyev OV, Paolucci S and Sen M. A multilevel wavelet collocation method for solving partial differential equations in a finite domain. *J Computat Phys* 1995; 120: 33–47.
14. Dai R and Cochran JJ. Wavelet collocation method for optimal control problems. *J Optimization Theory Appl* 2009; 143: 265–278.
15. Cai W and Wang J. Adaptive multiresolution collocation methods for initial boundary value problems of nonlinear PDEs. *SIAM J Numer Analysis* 1996; 33: 937–970.
16. Cai W and Zhang W. An adaptive spline wavelet ADI (SW-ADI) method for two-dimensional reaction-diffusion equations. *J Computat Phys* 1998; 139: 92–126.

17. Chui C and Wang J. On compactly supported spline wavelets and a duality principle. *Transact Am Math Soc* 1992; 330: 903–916.
18. Cohen A. *Numerical analysis of wavelet methods*. North-Holland: Elsevier, 2003.
19. Wie B. *Space vehicle dynamics and control*. Reston, Virginia: American Institute of Aeronautics and Astronautics, 2008.
20. Singhose W, Banerjee A and Seering W. Slewing flexible spacecraft with deflection-limiting input shaping. *J Guidance Control Dynamics* 1997; 20: 291–298.